

Finite-size scaling method for the Berezinskii-Kosterlitz-Thouless transition

Yun-Da Hsieh¹, Ying-Jer Kao¹ and A W Sandvik²

¹Center of Theoretical Sciences and Department of Physics,
National Taiwan University, No. 1, Sec. 4, Roosevelt Road, Taipei 10607, Taiwan

E-mail: yjkao@phys.ntu.edu.tw

² Department of Physics, Boston University, 590 Commonwealth Avenue,
Boston, Massachusetts 02215, USA

E-mail: sandvik@buphy.bu.edu

Abstract. We present an improved finite-size scaling method for reliably extracting the critical temperature T_{BKT} of a Berezinskii-Kosterlitz-Thouless (BKT) transition. Using the known Weber-Minhagen multiplicative logarithmic correction to the spin stiffness ρ_s at T_{BKT} and the Kosterlitz-Nelson relation between the transition temperature and the stiffness, $\rho_s(T_{\text{BKT}}) = 2T_{\text{BKT}}/\pi$, we define a size dependent transition temperature $T_{\text{BKT}}(L_1, L_2)$ based on a pair of system sizes L_1, L_2 , e.g., $L_2 = 2L_1$. We use Monte Carlo data for the standard two-dimensional classical XY model to demonstrate that this quantity is well behaved, rapidly convergent, and can be reliably extrapolated to the thermodynamic limit, $L_1, L_2 \rightarrow \infty$. Using GPU (graphical processing unit) computing, we obtain high-precision data for L up to 512 and extract a transition temperature $T_{\text{BKT}} = 0.89274(1)$, where the statistical error ± 1 in the last digit is about 6 times smaller than that of the best previous estimate.

PACS numbers: 64.60.De, 64.60.Bd, 64.60.fd

1. Introduction

The Berezinskii-Kosterlitz-Thouless (BKT) transition [1, 2, 3] is very well understood in terms of its physical mechanism of vortex-antivortex unbinding. The field-theoretical formulation of this two-dimensional (2D) problem of an U(1) symmetric order parameter gives a rigorous quantitative characterization of the transition into the critical (“quasi-ordered”) state obtaining below T_{BKT} . Despite this detailed understanding, analyzing numerical data (normally from Monte Carlo simulations) for the BKT transition on finite lattices still is considered a challenge [4, 5, 6, 7, 9, 10, 11], because of the presence of the Weber-Minhagen (WM) logarithmic finite-size corrections [12] to T_{BKT} and higher-order corrections to it [11].

We here propose an improved procedure to extract the BKT transition temperature in the thermodynamic limit using a finite-size definition of $T_{\text{BKT}}(L_1, L_2)$ based on the spin stiffness (helicity modulus) ρ_s for a pair of system sizes. This generalizes the “curve crossing” method often used when analyzing dimensionless quantities at conventional phase transitions [13], and also at the BKT transition [9, 11], but is even more powerful because we have combined it with the Nelson-Kosterlitz (NK) criterion [14] for the discontinuity of the stiffness in the thermodynamic limit,

$$\rho_s(T_{\text{BKT}}) = \frac{2T_{\text{BKT}}}{\pi}. \quad (1)$$

Imposing the constraint also for finite size, by adjusting the unknown constant appearing in the WM logarithmic correction, reduces the statistical fluctuations very significantly and leads to a well-behaved finite-size extrapolation.

1.1. Logarithmic corrections

WM derived the following logarithmic finite-size correction to the spin stiffness exactly at the transition temperature [12];

$$\rho_s(T_{\text{BKT}}, L) = \rho_s(T_{\text{BKT}}, \infty) \left(1 + \frac{1}{2 \ln(L) + C} \right), \quad (2)$$

where L is the linear system size and C an unknown constant which depends on the microscopic details of the system under study. We illustrate the slow convergence in Fig. 1 by plotting raw Monte Carlo results for ρ_s for the classical 2D XY model (we will describe the calculations below in Sec. 2) for different system sizes versus the temperature.

Previous approaches to use the WM correction in finite-size extrapolations of T_{BKT} have typically attempted to find the best value of C to fit a series of finite-size data [7], or by dividing out the factor containing the logarithm, with C chosen such that curves graphed versus the temperature for different system size cross each other within as narrow a range of T as possible (with the crossing points for large lattices approaching the BKT temperature) [9]. With the log-correction divided out, curves for different system sizes graphed versus T can also be scaled to collapse onto each other remarkably well by using the known exponential divergence of the correlation length [13].

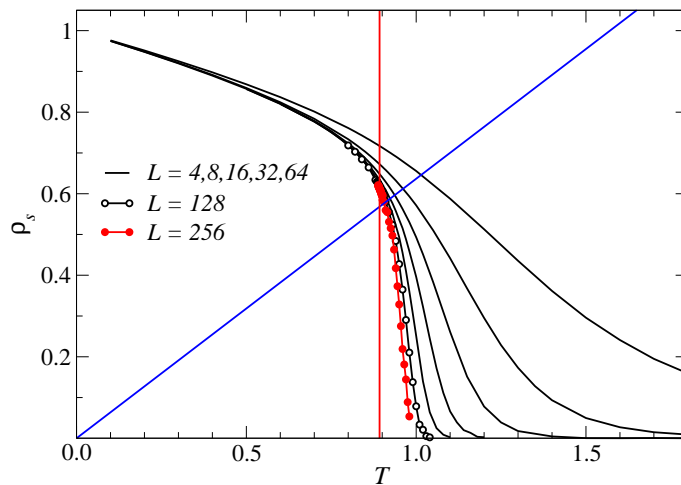


Figure 1. Monte Carlo results for the spin stiffness of the 2D classical XY model for several lattice sizes of the form $L = 2^n$. A discontinuity develops at T_{BKT} when $L \rightarrow \infty$, at a point satisfying the NK relation, Eq. (1), indicated here by the line $\rho_s = 2T/\pi$. The vertical line is the actual transition temperature $T_{\text{BKT}} \approx 0.89274$ (as determined in this paper) of the model. Thus, the stiffness discontinuity for $L \rightarrow \infty$ is located at the intersection of the two lines.

We here take a different route to finite-size extrapolations of T_{BKT} , by letting also C be size-dependent. For a pair of system sizes L_1, L_2 , we define $C(L_1, L_2)$ and consider the stiffness of the two sizes at arbitrary temperature T with the multiplicative correction in Eq. (2) divided out;

$$\rho_s^*(T, L_n) = \frac{\rho_s(T, L_n)}{1 + 1/[2 \ln(L_n) + C(L_1, L_2)]}, \quad n = 1, 2. \quad (3)$$

Clearly this quantity satisfies $\rho_s^*(T, L_n \rightarrow \infty) = \rho_s(T, \infty)$ and we can uniquely determine $C(L_1, L_2)$ and define a size-dependent transition temperature $T_{\text{BKT}}(L_1, L_2)$ by demanding that the normalized stiffness $\rho_s^*[T_{\text{BKT}}(L_1, L_2), L_n]$ for both $n = 1$ and $n = 2$ satisfies the NK relation (1). Thus, when plotted in the plane (ρ_s, T) , the quantities (3) for $n = 1$ and $n = 2$ will coincide at a point—in practice a point where the two curves cross each other—and this point is also exactly crossed by the NK line $\rho_s = 2T/\pi$. We illustrated the method with actual Monte Carlo data in Fig. 2. The size-dependence of the constant C , chosen to enforce the NK relation, changes the nature of the size corrections to the transition temperature. In Sec. 3 we will analyze the drift of the crossing point exemplified in Fig. 2 as a function of the system size with $L_1 = L$ and $L_2 = L/2$ and show that the size dependent temperature $T_{\text{BKT}}(L, L/2)$ converges very rapidly, almost linearly, with increasing L . It can be extrapolated to the thermodynamic limit using a low-order polynomial. We will also investigate the size dependence of the constant $C(L, L/2)$ in the logarithmic correction.

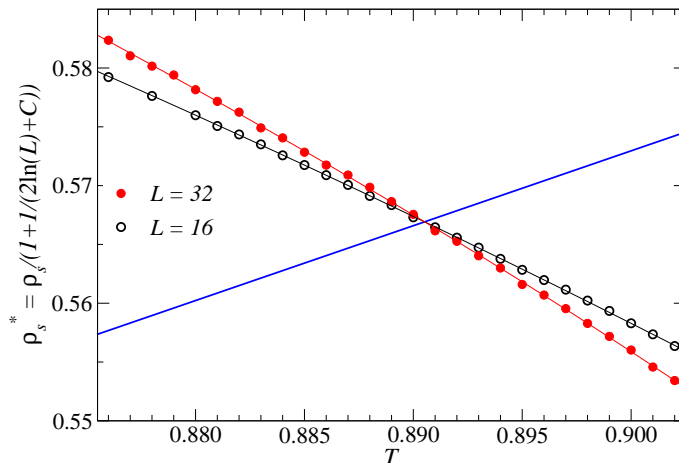


Figure 2. Illustration of the fitting procedure based on two system sizes; here with $L_1 = 16$ and $L_2 = 32$. The constant $C = C(L_1, L_2)$ in the logarithmic finite-size correction to the stiffness in Eq. (3) has been chosen such that the two ρ_s^* curves [where the log-correction in Eq. (2) has been divided out] cross each other exactly at the temperature satisfying the NK criterion, Eq. (1). In this case $C(16, 32) = 1.271$.

1.2. Stiffness renormalization

An interesting complication for finite-lattice calculations of ρ_s was noted some time ago by Prokof'ev and Svistunov [15]: For a system on a torus (i.e., with periodic boundary conditions in both directions of the 2D square lattice), the stiffness measured in the standard way in simulations [in the case of the classical XY model using Eq. (7) in Sec. 2] does not give ρ_s exactly. It is affected by a normalization factor depending on the aspect ratio $R = L_x/L_y$ of an $L_x \times L_y$ lattice. This is because the derivation of (7) based on imposing a twist (see, e.g., Ref. [13]) assumes that there is no net flux field threading the torus, while in fact such “field quanta” are thermally excited in the torus at any finite temperature, and they renormalize the stiffness in two dimensions (but there is no such effect in three dimensions). In the limit $L_x \rightarrow \infty, L_y \rightarrow \infty$, the stiffness measured according to (7) in the x and y direction is related to the stiffness ρ_s appearing in the BKT action and in Eqs. (1) and (2) according to;

$$\rho_x = f_x(R)\rho_s, \quad \rho_y = f_y(R)\rho_s, \quad (4)$$

where $f_x \neq f_y$ unless $R = 1$ and $f_x \rightarrow 1, f_y \rightarrow 0$ when $R \rightarrow \infty$.

Fortunately, the renormalization factors f_x, f_y due to the thermally excited flux quanta can be easily computed numerically (and in a special case analytically in terms of Ramanujan's Θ -function [7]); a list for selected R is given in Ref. [7]. Here we will use the aspect ratio $R = 1$, for which $f_x = f_y = 0.999825$ [15]. As previously noted in Ref. [7], Monte Carlo calculations of T_{BKT} have in the past typically not reached the level of precision where this factor would play any role (for $R = 1$, which is normally used), but in high-precision calculations the renormalization should be included in order to avoid a systematical error. Our calculations here are at the level where the renormalization must be taken into account, as was also done in a recent large-scale study [10].

2. Monte Carlo calculations

We use standard Monte Carlo methods implemented using GPU computing to calculate the stiffness (helicity modulus) for the standard classical XY model (two-dimensional vectors of size $S = 1$) with energy

$$H = - \sum_{\langle ij \rangle} \vec{S}_i \cdot \vec{S}_j = - \sum_{\langle ij \rangle} \cos(\Theta_i - \Theta_j), \quad (5)$$

where the expression in terms of the angles Θ_i is more convenient in practice. We here first discuss the definition of the helicity modulus and then discuss some details of the Monte Carlo algorithms and their GPU implementation.

2.1. The helicity modulus

The helicity modulus is defined according to

$$\rho_a = \frac{1}{N} \left. \frac{\partial^2 F(\phi)}{\partial \phi^2} \right|_{\phi=0}, \quad (6)$$

where $F(\phi)$ is the free energy in the presence of a twist field (or, equivalently, a twisted boundary condition) in the lattice direction a ($a = x, y$). The Monte Carlo estimator for this quantity is given by

$$\rho_a = \frac{1}{L^2} \left(\langle H_a \rangle - \frac{1}{T} \langle I_a^2 \rangle \right), \quad (7)$$

where H_a is the energy including only the a -directed links (nearest-neighbor site pair) in (5) and I_a is the “current” in the a direction, given by

$$I_a = - \sum_{\langle i,j \rangle_a} \sin(\Theta_j - \Theta_i). \quad (8)$$

A pedagogical derivation of these expressions can be found in Ref. [13]. Note again that the stiffness constant appearing in the BKT action is related to the helicity moduli ρ_x, ρ_y (where we use $L_x = L_y$ so that $\rho_x = \rho_y$) by the renormalization factors in (4).

2.2. GPU computing

Here we summarize our Monte Carlo simulations on the GPU, which we have implemented using the NVIDIA CUDA framework. We refer interested readers to available literature for an introduction to the details of the GPU hardware and the programming models [16].

We use parallel Metropolis single-spin flips as well as over-relaxation moves [17, 18]. In addition, to improve the dynamics, and for convenience when computing stiffness values for a range of temperatures close to the transition, we run several temperatures and apply parallel-tempering (PT) [19], where configurations for nearby temperatures are occasionally swapped (using the Metropolis acceptance probability). One Monte Carlo step (MCS) is then defined as one Metropolis sweep, an over-relaxation sweep of

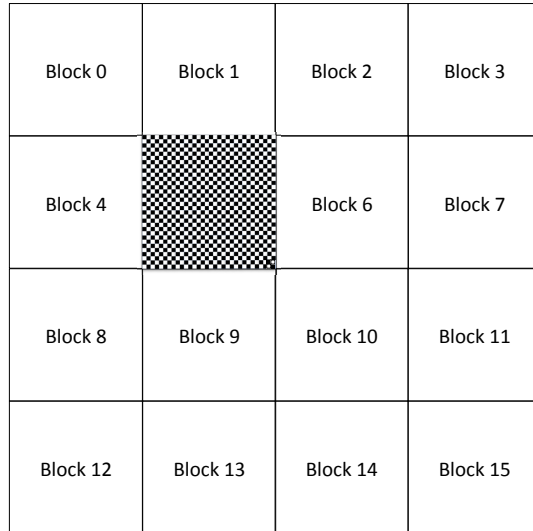


Figure 3. Mapping of a 128×128 lattice to thread blocks on GPU. Each thread block of $16 \times 16 = 256$ threads performs updates on $32 \times 32 = 1024$ spins.

the entire lattice, followed by one parallel-tempering exchange attempt for each pair of adjacent temperatures.

To implement the parallel Metropolis and over-relaxation updates in a way suitable for the GPU, we divide the entire lattice into blocks of $32 \times 32 = 1024$ spins. Each block is decomposed into two different sub-lattices, as shown in Fig. 3. Each block is assigned to a *thread block* [16] containing $16 \times 16 = 256$ threads, which execute the same GPU *kernel* in parallel [16]. Each thread is responsible for updating $2 \times 2 = 4$ spins, with two “black” sites and two “white” sites, so that there are enough arithmetic operations to hide the latency of the global memory accesses [16]. We apply the checkerboard decomposition algorithm to perform the Metropolis single-spin flips in parallel [20, 21]. We first update all the black spins in parallel via a GPU kernel. After all the black spins belonging to different blocks are updated, another kernel is launched to update all the white spins.

Due to the special architecture of the GPU, the commonly used Mersenne-Twister (MT) random number generator (RNG) can not be efficiently implemented at the thread level. Instead, we use a faster RNG implementation specially designed for the GPU architecture, the *Warp Generator* [22]. We note that although it has a smaller period of $2^{1024} - 1$ than MT ($2^{19937} - 1$), we do not find any noticeable statistical bias compared with the CPU runs using the MT.

It is well established that the single-spin flip Metropolis update suffers from critical slowing down near phase transitions and for increased efficiency one has to resort to cluster updates [23, 24]. However, GPU implementations of the cluster update are complicated and less efficient [25]. We instead implemented the microcanonical over-relaxation update [17, 18] and found it to be as efficient as the cluster update in reducing slowing-down. It should also be noted that slowing-down is not very serious at the BKT transition compared to standard critical points.

In an over-relaxation move, the new spin direction on site i is obtained by reflecting it with respect to its local molecular field, $\mathbf{H}_i = -\sum_{\langle ij \rangle} \mathbf{S}_j$, according to

$$\mathbf{S}'_i = -\mathbf{S}_i + 2 \frac{\mathbf{S}_i \cdot \mathbf{H}_i}{H_i^2} \mathbf{H}_i. \quad (9)$$

This update maps the system from a point in the phase space to another point with exactly the same energy. After several sweeps, the system is able to explore a larger region of the phase space without being stuck at a particular local minimum for a long time, thus improving the ergodicity of the simulation.

To better equilibrate the simulations and further reduce slowing-down effects close to the transition, we also perform PT sweeps [19] on many systems at different temperatures simulated simultaneously. After a certain number of MCSs (often just one), we swap two adjacent configurations X_m, X_n at neighboring temperatures T_m, T_n with the acceptance probability of

$$W(X_m, T_m | X_n, T_n) = \min [1, e^{(1/T_m - 1/T_n)(E_m - E_n)}], \quad (10)$$

where E_n is the total energy of replica n .

To reduce the amount of data transfer between the CPU and the GPU, we store all the spin configurations at different temperatures in the GPU global memory, and all updates are performed through the kernel functions on the GPU. Measurements are also performed on the GPU and the results are sent back to the CPU for binning. Simulations were carried out at 21 temperatures ranging from $T = 0.888$ to $T = 0.898$ for system sizes ranging from $L = 16$ to $L = 512$ in steps of 16 (to keep optimal sizes for the GPU memory structure, as illustrated in Fig. 3). In each simulation, about 1.2×10^8 measurements were made after 10^6 MCSs for equilibration. The data were blocked into bins of 10^5 measurements, which were subject to further analyses post-simulation. The simulations were performed on Tesla C2090 GPUs, and took approximately 3600 GPU hours for producing the whole data set discussed in this paper.

We also used standard CPUs with single-spin and cluster updates for small systems. For the range of systems where we have results from both CPU and GPU calculations, they agree perfectly within statistical errors.

3. Results

We here use system pairs of the form $(L, L/2)$ and extract crossing points such as the one shown in Fig. 2. Note again that the constant C in Eq. (3) depends on L but for large L it must converge to an asymptotic value (which depends on the microscopic details of the model). We here first discuss a few more details of the fitting procedures and then study the convergence properties of the transition temperature and the constant C .

3.1. Fitting procedures

To systematically carry out the analysis illustrated in Fig. 2, we fit a polynomial (typically of second-order) to a range of Monte Carlo data for the two system sizes

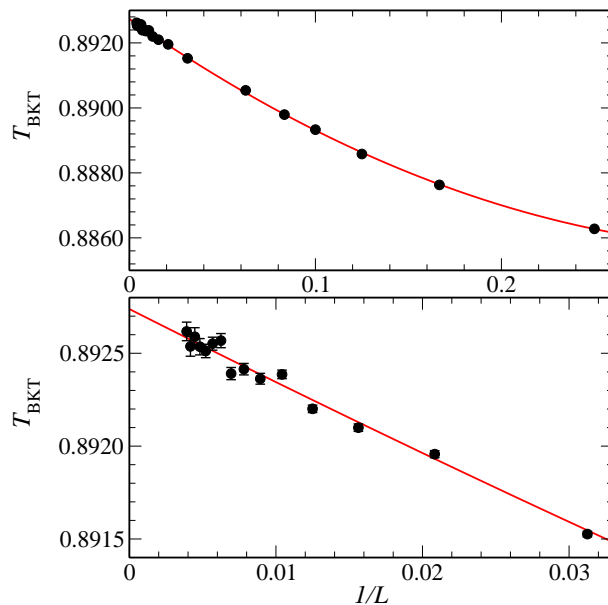


Figure 4. The finite-size transition temperature extracted on the basis of system-size pairs $(L/2, L)$ versus $1/L$. The curve is a second-order polynomial fitted to all the data points, giving the infinite-size extrapolated value of the transition temperature $T_{\text{BKT}} = 0.89274(1)$, where the number within parenthesis indicates the statistical error of the last digit. The lower panel shows is a zoom-in of the large-size data.

close to the transition. The crossing point is extracted using the polynomials, and the deviation of the stiffness constant from the NK value (including the renormalization factor discussed in Sec. 1.2) is recorded. A sweep of such fitting procedures is carried out to minimize the NK deviation, which can be done to machine precision. Error bars are computed by repeating this procedure for a large number (hundreds) of bootstrap samples of the data.

3.2. Transition temperature

Fig. 4 shows our results for $T_{\text{BKT}}(L, L/2)$, for system sizes in the range $L = 4$ to 512. A second-order polynomial gives a statistically sound fit to all the data, and removing small system sizes does not affect the extrapolated $L \rightarrow \infty$ value. The size dependence is weak and essentially linear, with a very small quadratic correction required when including small sizes in the fit. Naturally, the standard deviation of the extrapolated result increases as the data set becomes smaller. For example, including all the data points starting from $L = 4$ we obtain $T_{\text{BKT}} = 0.89274(1)$, where the number within parenthesis is the standard deviation of the preceding digit. Starting instead from $L = 32$ we obtain $T_{\text{BKT}} = 0.89275(2)$. These numbers agree within statistical errors and the quality of the fit is very similar in the two cases. There is, thus, no reason to exclude the small sizes, and we present $T_{\text{BKT}} = 0.89274(1)$ as our final result for the transition temperature. To our knowledge, the best previous result, obtained recently in a large-scale GPU study with system sizes up to $L = 16384$ was $T_{\text{BKT}} = 0.89289(6)$,

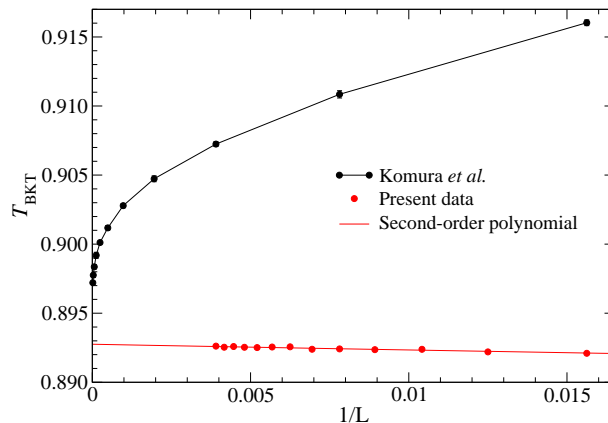


Figure 5. Comparison of our finite-size estimates of T_{BKT} (with the second-order polynomial fit shown as well) and those of Ref. [10] (where the lines between data points only provide a guide to the eye).

which deviates from our result by about 2.5 standard deviations. i.e., the calculations are marginally consistent with each other.

To further demonstrate how our calculation leads to a significantly more precise value (reducing the statistical error by a factor of 6), even though much smaller systems were used, we compare our finite-size data directly with those of Ref. [10] in Fig. 5. Note that the finite-size definitions of T_{BKT} are different in the two calculations, and that the data of Ref. [10] were originally analyzed in a different way, with a logarithmic correction (adjusted for the best fit to the data) to the infinite-size T_{BKT} . The comparison is still very illuminating. It is clear that our definition has much smaller size corrections, and also that the corrections in the data of [10] cannot be captured by a polynomial (hence the different method of analysis in Ref. [10]). The statistically marginal agreement between the two extrapolations could be due to neglected higher-order logarithmic corrections neglected in Ref. [10] (which, we have argued, are taken into account implicitly in our work by the size-dependent constant C).

3.3. The constant C

The very rapid, asymptotically linear convergence of our finite-size data suggests that the method of letting the constant C in Eq. (2) be size-dependent effectively captures (or eliminates) higher-order logarithmic corrections [11] to the WM form. It is then also interesting to examine the convergence of C . The results are shown in Fig. 6. Here the results cannot be well described by a low-order polynomial when small system sizes are excluded. All data points can be fitted to the form $a + b \cdot e^{-cx}(1 + dx + ex^2)$, where $x = 1/L$. This is the form shown in the figure. For extrapolating to infinite size, a quadratic polynomial in the range where it works gives the same result as the exponential form above; $C = 2.12(3)$.

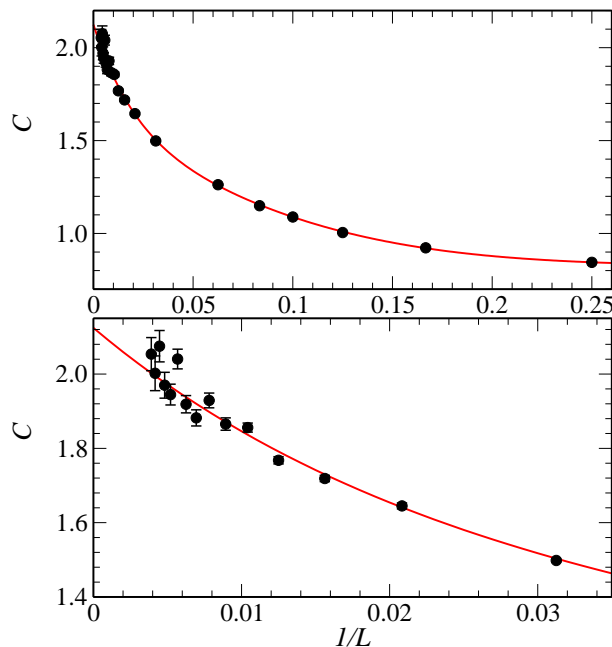


Figure 6. Size dependence of the constant C in the WM logarithmic correction used in Eq. (3), computed using system-size pairs $(L/2, L)$. The continuous curve is a fit of the form discussed in the main text. The upper panel shows all the data used in the analysis and the lower panel focuses on the larger systems.

4. Summary

We have presented an improved finite-size scaling method for studying the BKT transition. Taking advantage of the NK relationship governing the spin stiffness at T_{BKT} in the thermodynamic limit, we defined a two-size estimate (curve-crossing) for the transition temperature which is constrained by this relationship also for finite size. We tested the procedure for the standard 2D XY model, with high-precision finite-size data obtained by Monte Carlo simulations on GPUs on system sizes up to 512×512 . The results exhibit a very rapid, almost linear convergence of T_{BKT} , and the extrapolated value $T_{\text{BKT}} = 0.89274(1)$ is, to our knowledge, the most precise estimate so far for this model. We anticipate that our scaling method should be the preferred way to extract T_{BKT} in general.

Note that the form (2) of the logarithmic correction is asymptotically valid only exactly at $T = T_{\text{BKT}}$ [12], but that does not invalidate our use of it at any temperature for the purpose of a procedure to analyze finite-size data. Since the crossing points tend to $T_{\text{KT B}}$ in the thermodynamic limit, the assumptions underlying the use of (3) in combination with the NK criterion are guaranteed to hold asymptotically. Whether or not the actual higher-order corrections to (2) can be described well with a size dependent C (i.e., the remaining size dependence of T_{BKT} is weak), the procedure is unbiased in the limit $L \rightarrow \infty$. The fact that results for T_{BKT} depends only weakly on the system size, and can be described by a low-order polynomial, strongly suggests that the size dependent C does capture the higher-order corrections very well. While

we have not formally proved that the size-dependent constant C (in combination the NK relationship) eliminates logarithmic corrections, the fact that our data can be well described with a very simple form without logarithms strongly suggests it. It would be interesting to test these numerical results also based on the renormalization-group treatment of the BKT transition.

Acknowledgments

This work was supported by NSC in Taiwan through Grant No. 100-2112-M-002-013-MY3 (YDH and YJK), NTU Grant number 101R891004 (YJK), and by the NSF under Grants No. DMR-1104708 and PHY-1211284 (AWS). AWS also gratefully acknowledges support from the NCTS in Taipei for visits to National Taiwan University.

References

- [1] V. L. Berezinskii, *Sov. Phys. JETP* **34** (1972) 610.
- [2] J. M. Kosterlitz and D. J. Thouless, *J. Phys. C* **6** (1973) 1181.
- [3] J. M. Kosterlitz, *J. Phys. C* **7** (1974) 1046.
- [4] N. Schultka and E. Manousakis, *Phys. Rev. B* **49** (1994) 12071.
- [5] N. Schultka and E. Manousakis, *Phys. Rev. B* **51** (1995) 11712.
- [6] Y. Tomita and Y. Okabe, *Phys. Rev. B* **65** (2002) 184405.
- [7] R. G. Melko, A. W. Sandvik, and D. J. Scalapino, *Phys. Rev. B* **69** (2004) 014509.
- [8] M. Hasenbusch, *J. Phys. A: Math. Gen.* **38** (2005) 5869.
- [9] J. Carrasquilla and M. Rigol, *Phys. Rev. A* **86** (2012) 043629.
- [10] Y. Komura and Y. Okabe, *J. Phys. Soc. Jpn.* **81** (2012) 113001.
- [11] J. Iaconis, S. Inglis, A. B. Kallin, and R. G. Melko, arXiv:1210.2403.
- [12] H. Weber, P. Minnhagen, *Phys. Rev. B* **37** (1987) 5986.
- [13] A. W. Sandvik, *AIP Conf. Proc.* **1297** (2010) 135 (2010); arXiv:1101.3281.
- [14] D. R. Nelson, J. M. Kosterlitz, *Phys. Rev. Lett.* **39** (1977) 1201.
- [15] N. V. Prokof'ev and B. V. Svistunov, *Phys. Rev. B* **61** (2000) 11282.
- [16] http://www.nvidia.com/object/cuda_home_new.html.
- [17] M. Creutz: *Phys. Rev. D* **36** (1987) 515.
- [18] Y. H. Li and S. Teitel: *Phys. Rev. B* **40** (1989) 9122.
- [19] K. Hukushima and K. Nemoto: *J. Phys. Soc. Jpn.* **65** (1996) 1604.
- [20] T. Preis, P. Virnau, W. Paul, and J. J. Schneider: *J. Comp. Phys.* **228** (2009) 4468.
- [21] M. Weigel: *Computer Physics Communications* **182** (2011) 1833.
- [22] http://cas.ee.ic.ac.uk/people/dt10/research/rngs-gpu-warp_generator.html.
- [23] R. H. Swendsen and J.-S. Wang: *Phys. Rev. Lett.* **58** (1987) 86.
- [24] U. Wolff: *Phys. Rev. Lett.* **62** (1989) 361.
- [25] M. Weigel, arXiv:1105.5804v2.